

The impact of input signal deformation on atan2 angle calculation error

Mitja Alič

Faculty of Electrical Engineering, University of Ljubljana, Tržaška cesta 25, 1000 Ljubljana
E-mail: mitja1357@gmail.com

The output of position sensors such as encoders and resolvers is a pair of quadrature sine and cosine signals. Angle calculation can be done with atan2 function. Due to improper installation of sensor, sine and cosine signal can be deformed. In that case calculated angle includes error. Error was analyzed for non-equal amplitudes, non-orthogonality, DC offset and common mode signal. Error was analyzed in frequency specter, that yielded a function of error based on input signal deformation. Error is presented in Fourier series form.

1 Introduction

High quality motor regulation is present in numerous applications and become unavoidable. For a consistent and reliable measurement of rotation, position sensors are used [1], such as encoders and resolvers [2][3][4]. Because the output of such sensors is a pair of quadrature sine and cosine signals, angle must first be calculated. The easiest way of doing so is by directly calculating atan2, which returns a value between $[-\pi, \pi]$.

Position sensors are not ideal, their acquired sine and cosine signal can be deformed, phase shifted and DC offset. All of these imperfections cause the calculated angle to also include error.

Literature [5], [6], [7] and [8] analyses the impact of such imperfection for lower harmonics only and states that error of imperfections scale linearly. During our research we found, that the error specter also contains higher harmonics. The paper examines error waveform dependent on input signal mismatch with Fourier analysis.

2 Methodology and results

Output from a position sensor can be represented with

$$\text{Sin} = B_0 + B_1 \sin(\theta + \varphi_s) + \text{CMM} \quad (1)$$

$$\text{Cos} = A_0 + A_1 \cos(\theta + \varphi_c) + \text{CMM} \quad (2)$$

Where B_0 and A_0 represent DC offset, B_1 and A_1 signal amplitude, φ_s and φ_c phase shift and θ reference angle. Signals (1) and (2) can also have a common superimposed AC signal represented as CMM (3). CMM can be of cosine or sine form with Δ_c and Δ_s as amplitude.

$$\text{CMM} = \Delta_c \cos(\theta) + \Delta_s \sin(\theta) \quad (3)$$

By calculating atan2 for eq. (1) and (2)

$$\varphi = \text{atan2}(\text{Sin}, \text{Cos}) \quad (4)$$

and then subtract (4) from an unaltered signal

$$\varepsilon = \varphi - \text{atan2}(\sin(\theta), \cos(\theta)) \quad (5)$$

error based on deformation parameter. Because AC signal analysis is simpler in frequency domain, error was converted with Fast Fourier Transform. By varying each parameter individually we examined the impact of the parameter in question on specter of error. Output of atan2 was examined by sending each parameter in eq. (1) and (2) to infinity or worst case with phase shift. In this case amplitude and phase of each harmonic approaches to a limit value.

Amplitude and phase of error in dependence on the changing parameter were approximated by a function, that best suited numerical waveform obtained from the error spectrum. The set of functions decreases by checking the limit value to which each amplitude and phase approach. We were looking for the best approximation with polynomials, rational functions, exponential, trigonometric and cyclometric functions. The best approximation was sought using the minimum squares method.

2.1 Error definition at amplitude mismatch

In the first case was observed the impact of different amplitudes on error. The output of the atan2 function is determined by the eq. (1) and (2) quotient. Since only the ratio of the amplitudes needs to be preserved, we multiplied both signals by $\frac{1}{A_1}$. By changing only the amplitudes in (1) and (2), input signals are:

$$\text{Sin} = k \sin(\theta), \quad (6)$$

$$\text{Cos} = \cos(\theta), \quad (7)$$

where k represents $\frac{B_1}{A_1}$.

By varying the parameter k from 0 to infinity, it was found that, the error specter consists of even harmonics only. It was also observed that phase shift did not change. When k approaches infinity, the amplitude of harmonics

approaches $\frac{180}{\pi} \frac{2}{n}$, where n represents n -th harmonic. Eq. (8) which contains even harmonics only.

$$\varepsilon(k \rightarrow \infty) = \frac{180}{\pi} \sum_{n=1}^{\infty} \frac{1}{n} \sin 2n\theta \quad (8)$$

Because second harmonic is the largest, we approximated it first (Figure 1).

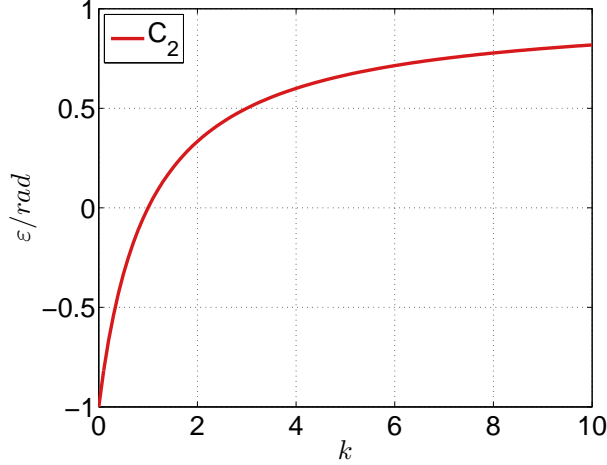


Figure 1: Waveform of the second harmonic depending on k

Best approximation was rational function (9), with summed squared error (SSE) $1.18 \cdot 10^{-10}$ degrees.

$$C_2(k) = \frac{180}{\pi} \cdot \frac{k-1}{k+1} \quad (9)$$

It was assumed, that higher order harmonics were correlated with base harmonic. Function, that describes error depending on k is presented in Fourier series form (10).

$$\varepsilon(k) = \frac{180}{\pi} \sum_{n=1}^{\infty} \frac{1}{n} \left(\frac{k-1}{k+1} \right)^n \sin 2n\theta \quad (10)$$

By replacing k with ratio of amplitudes $\frac{B_1}{A_1}$, we get final equation

$$\varepsilon(A_1, B_1) = \frac{180}{\pi} \sum_{n=1}^{\infty} \frac{1}{n} \left(\frac{B_1 - A_1}{B_1 + A_1} \right)^n \sin 2n\theta, \quad (11)$$

which is valid for positive ratio of amplitudes only.

$$\frac{B_1}{A_1} \geq 0.$$

2.2 Error definition at non-orthogonality

In second case, it was examined the impact of phase deformation. Input signals are represented as:

$$\sin = \sin(\theta + \varphi_s) \quad (12)$$

$$\cos = \cos(\theta + \varphi_c) \quad (13)$$

Error was analyzed for φ_s and φ_c individually, in the end equations were combined.

Worst case of error is, when φ_s approaches 90° and can be presented as Fourier series (14). Error consists of DC component and even harmonics only.

$$\varepsilon(\varphi_s \rightarrow 90^\circ) = 45^\circ - \frac{180}{\pi} \sum_{n=1}^{\infty} \frac{1}{n} \sin(2n\theta) \quad (14)$$

Correlation between amplitudes and φ_s yields tangent function (Figure 2). DC component and phase of error were being changed linearly. Tangent function approximate second harmonic with SSE of $1.18 \cdot 10^{-10}$ degrees.

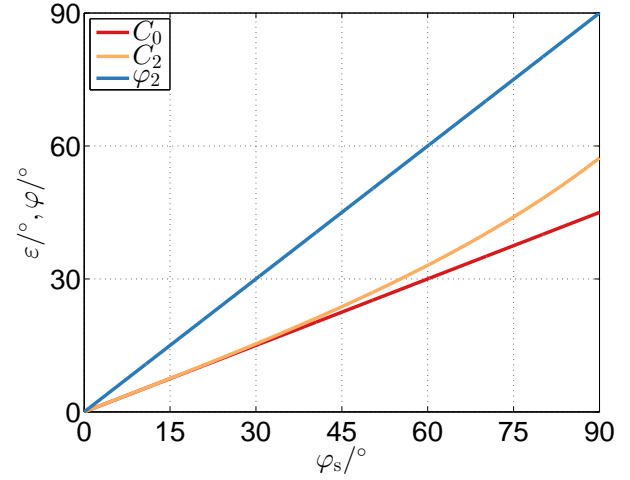


Figure 2: Waveforms of DC component C_0 , amplitude of second harmonic C_2 and phase of second harmonic φ_2 compared to ideal cosine signal, due to phase shift φ_s

Same procedure can be applied for parameter φ_c as well. Errors from (12) and (13) are independent and their contribution can be combined into (15).

$$\begin{aligned} \varepsilon(\varphi_s, \varphi_c) &= \frac{\varphi_s + \varphi_c}{2} + \\ &+ \frac{180}{\pi} \sum_{n=1}^{\infty} \frac{1}{n} \left(\tan \frac{\varphi_s - \varphi_c}{2} \right)^n \sin(2n\theta + n(90^\circ + \varphi_s + \varphi_c)) \end{aligned} \quad (15)$$

Expression (15) is valid only for range:

$$\varphi_s - \varphi_c \in [-90^\circ, 90^\circ]$$

2.3 Error definition at DC component in one input signal only

By varying DC component in (1) and (2) equations are:

$$\sin = \sin(\theta) + B_0 \quad (16)$$

$$\cos = \cos(\theta) + A_0. \quad (17)$$

When parameter A_0 approaches infinity, error is described by eq. (18).

$$\varepsilon(A_0 \rightarrow \infty) = \frac{180}{\pi} \sum_{n=1}^{\infty} \frac{2}{n} \sin(n\theta + n180^\circ). \quad (18)$$

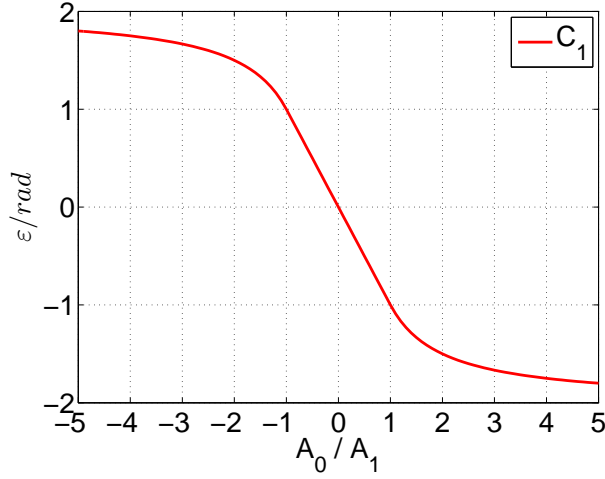


Figure 3: Amplitude of first harmonic depending on $\frac{A_0}{A_1}$

Error does not contain DC component and the highest harmonic is the first. The waveform from figure 3, was split into 3 parts based on ratio between offset and amplitude. Expression which best approximates waveform of first harmonic of error with SSE of $1.21 \cdot 10^{-7}$ degrees is in exponential and linear form (19):

$$\varepsilon(A_0, A_1) = \begin{cases} \frac{180}{\pi} \sum_{n=1}^{\infty} \frac{1}{n} (2 - |\frac{A_0}{A_1}|^{-n}) \sin(n\theta), & \frac{A_0}{A_1} \leq -1 \\ \frac{180}{\pi} \sum_{n=1}^{\infty} (-1)^n \frac{1}{n} (\frac{A_0}{A_1})^n \sin(n\theta), & |\frac{A_0}{A_1}| \leq 1 \\ \frac{180}{\pi} \sum_{n=1}^{\infty} (-1)^n \frac{1}{n} (2 - (\frac{A_0}{A_1})^{-n}) \sin(n\theta), & \frac{A_0}{A_1} \geq 1 \end{cases} \quad (19)$$

Same procedure can be applied for parameter B_0 as well. Result is eq. (20).

$$\varepsilon(B_0, B_1) = \begin{cases} \frac{180}{\pi} \sum_{n=1}^{\infty} \frac{1}{n} (2 - |\frac{B_0}{B_1}|^{-n}) \sin(n\theta - 90^\circ n), & \frac{B_0}{B_1} \leq -1 \\ \frac{180}{\pi} \sum_{n=1}^{\infty} \frac{1}{n} (\frac{B_0}{B_1})^n \sin(n\theta + 90^\circ n), & |\frac{B_0}{B_1}| \leq 1 \\ \frac{180}{\pi} \sum_{n=1}^{\infty} \frac{1}{n} (2 - (\frac{B_0}{B_1})^{-n}) \sin(n\theta + 90^\circ n), & \frac{B_0}{B_1} \geq 1 \end{cases} \quad (20)$$

2.4 Error definition at common DC component in both input signals

Input signals can also contain common DC component. This happens when resolvers stator coils are improperly install. Same analysis as in subsection 2.3 can be applied in this case as well. Result is presented in eq. (21).

$$\varepsilon(A_0, B_0 = A_0, A_1) = \begin{cases} \frac{180}{\pi} \sum_{n=1}^{\infty} \frac{1}{n} (2 - |\sqrt{2} \frac{A_0}{A_1}|^{-n}) \sin(n\theta - 45^\circ n), & \frac{A_0}{A_1} \leq -\frac{\sqrt{2}}{2} \\ \frac{180}{\pi} \sum_{n=1}^{\infty} \frac{1}{n} (\sqrt{2} \frac{A_0}{A_1})^n \sin(n\theta + 135^\circ n), & |\frac{A_0}{A_1}| \leq \frac{\sqrt{2}}{2} \\ \frac{180}{\pi} \sum_{n=1}^{\infty} \frac{1}{n} (2 - (\sqrt{2} \frac{A_0}{A_1})^{-n}) \sin(n\theta + 135^\circ n), & \frac{A_0}{A_1} \geq \frac{\sqrt{2}}{2} \end{cases} \quad (21)$$

2.5 Impact of CMM signal on error

CMM signal is the result of improper resolvers rotor part installation.

By limiting error of Δ_c to infinity. Because CMM effects amplitude mismatch and non-orthogonality of input signals, error was expected to contain DC component and even harmonics only. Error when Δ_c approaches infinity, is presented in (22).

$$\varepsilon(\Delta_c \rightarrow \infty) = 45^\circ - \frac{180}{\pi} \sum_{n=1}^{\infty} \frac{1}{n} \sin(2n\theta). \quad (22)$$

Because general approximation was not found, error specter was split into sine and cosine part (23).

$$C_{ns}(\Delta_c) \cdot \sin(n\theta) + C_{nc}(\Delta_c) \cdot \cos(n\theta) \quad (23)$$

Figure 4 presents split second harmonic and DC component.

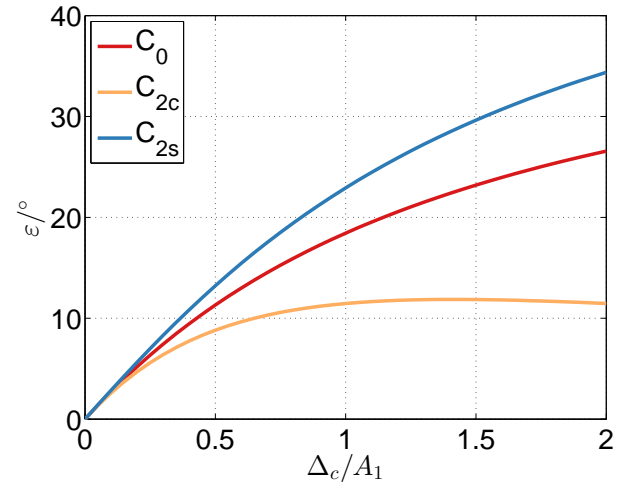


Figure 4: Waveform of DC component and split second harmonic depending on $\frac{\Delta_c}{A_1}$

DC component was approximated with SSE of $1.94 \cdot 10^{-22}$ degrees with atan function. Waveform of C_{2s} and C_{2c} were approximated with SSE to less then $1.15 \cdot 10^{-9}$ degrees. Final function, that described error depending on Δ_c is presented in Fourier series form (24).

$$\varepsilon(A_1, \Delta_c) = \text{atan} \frac{\Delta_c}{\Delta_c + 2A_1} + \frac{180}{\pi} \sum_{n=1}^{\infty} \frac{1}{n} \left(\frac{\Delta_c}{\sqrt{\Delta_c^2 + 2A_1\Delta_c + 2A_1}} \right)^n \sin(2n\theta + n(90^\circ + \text{atan}(\frac{\Delta_c + A_1}{A_1}))) \quad (24)$$

Same procedure can be applied for parameter Δ_s as well. Result is eq.(25)

$$\varepsilon(A_1, \Delta_s) = -\text{atan} \frac{\Delta_s}{\Delta_s + 2A_1} + \frac{180}{\pi} \sum_{n=1}^{\infty} \frac{1}{n} \left(\frac{\Delta_s}{\sqrt{\Delta_s^2 + 2A_1\Delta_s + 2A_1}} \right)^n \sin(2n\theta + n(90^\circ - \text{atan}(\frac{\Delta_s + A_1}{A_1}))) \quad (25)$$

Eq. (24) and (25) are valid for only:

$$\Delta_s, \Delta_c > -A_1$$

3 Comment on results

After determining approximated error functions (11) (15) (19) (20) (21) (24) (25), the error difference was analyzed against (5). Approximated functions were defined with Fourier series, with the first 20 components. Difference between calculated error in (11) and error in (5) is presented in figure 5, where $A_1 = 1$ and $B_1 = 1.1$ were used. Approximation fault is in the vicinity of a numeric error. A comparison of the errors in the frequency spectrum showed a minimum deviation between harmonics of the same frequency.

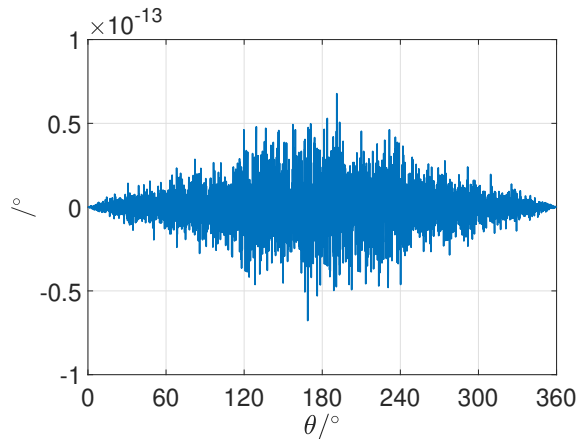


Figure 5: Difference between predicted (11) and actual error (5)

4 Conclusion

With methods described in this paper improper installation of encoders and resolvers can be uncovered. By analyzing full specter of angle error, contribution of individual harmonics can be observed. The influence of signal mismatch, non-orthogonality, DC offset and common mode signal is studied in the spectrum of the angle error.. This paper extends findings of literature by exploring larger deformations with a more accurate approximation of whole specter.

Input signals can also include higher harmonics distortion, which was not examined in this paper.

Individual errors cannot be summed up, because obtained approximations of errors are interdependent. Function that define error for all deformations in (1) and (2) and impact of high harmonics distortion is a challenge for further work.

Acknowledgment

This paper could not be possible without the help of my friend and colleague Draž Kunšič. I am deeply grateful for his generous help and encouragement.

References

[1] Gachter J., Hirz M., Seebacher R., "Impact of Rotor Position Sensor Errors on Speed Controlled Permanent Magnetized Synchronous Machines", IEEE 12th International

Conference on Power Electronics and Drive Systems (PEDS), pp.822-830, 12-15 Dec. 2017

[2] Brugnano F., Concari C., Imamovic E., Savi F., Toscani A., Zanichelli R., "A simple and accurate algorithm for speed measurement in electric drives using incremental encoder", IECON 2017 - 43rd Annual Conference of the IEEE Industrial Electronics Society, pp. 8551-8556, 29 Oct.-1 Nov. 2017

[3] Reddy B.P., Murali A., Shaga G., "Low Cost Planar Coil Structure for Inductive Sensors to Measure Absolute Angular Position", 2017 2nd International Conference on Frontiers of Sensors Technologies (ICFST), pp.14-18, 14-16 April 2017

[4] Zhang Z., Ni F., Liu H., Jin M., "Theory analysis of a new absolute position sensor based on electromagnetism", International Conference on Automatic Control and Artificial Intelligence, pp.2204-208, 3-5 Mar. 2012

[5] Lara J., Chandra A., "Position Error Compensation in Quadrature Analog Magnetic Encoders through an Iterative Optimization Algorithm", IECON 2014 - 40th Annual Conference of the IEEE Industrial Electronics Society, pp.3043-3048, 29 Oct.-1 Nov. 2014

[6] Qi Lin, T. Li, Z. Zhou, "Error Analysis and Compensation of the Orthogonal Magnetic Encoder", Proceedings of IEEE ICMCC Conference, pp.11-14, 21-23 Oct. 2011

[7] Hanselman D.C., "Resolver Signal Requirements for High Accuracy Resolver-to-Digital Conversion", IEEE Transactions on Industrial Electronics, vol.37, no.6, pp.556-561, Dec. 1990

[8] Demierre M., "Improvements of CMOS Hall Microsystems and Application for Absolute Angular Position Measurements", PhD. thesis, pp. 152-161, Federal Polytechnic School of Lausanne, Switzerland, 2003